



PULasso: High-dimensional variable selection with presence-only data

Hyebin Song & Garvesh Raskutti

To cite this article: Hyebin Song & Garvesh Raskutti (2018): PULasso: High-dimensional variable selection with presence-only data, Journal of the American Statistical Association, DOI: [10.1080/01621459.2018.1546587](https://doi.org/10.1080/01621459.2018.1546587)

To link to this article: <https://doi.org/10.1080/01621459.2018.1546587>



View supplementary material [↗](#)



Accepted author version posted online: 13 Dec 2018.



Submit your article to this journal [↗](#)



Article views: 41



View Crossmark data [↗](#)

PULasso: High-dimensional variable selection with presence-only data

Hyebin Song

Department of Statistics, University of Wisconsin-Madison
and

Garvesh Raskutti *

Department of Statistics, University of Wisconsin-Madison

October 12, 2018

Abstract

In various real-world problems, we are presented with classification problems with *positive and unlabeled data*, referred to as presence-only responses. In this paper, we study variable selection in the context of presence only responses where the number of features or covariates p is large. The combination of *presence-only responses* and *high dimensionality* presents both statistical and computational challenges. In this paper, we develop the *PULasso* algorithm for variable selection and classification with positive and unlabeled responses. Our algorithm involves using the majorization-minimization (MM) framework which is a generalization of the well-known expectation-maximization (EM) algorithm. In particular to make our algorithm scalable, we provide two computational speed-ups to the standard EM algorithm. We provide a theoretical guarantee where we first show that our algorithm converges to a stationary point, and then prove that any stationary point within a local neighborhood of the true parameter achieves the minimax optimal mean-squared error under both strict sparsity and group sparsity assumptions. We also demonstrate through simulations that our algorithm outperforms state-of-the-art algorithms in the moderate p settings in terms of classification performance. Finally, we demonstrate that our PULasso algorithm performs well on a biochemistry example.

Keywords: PU-learning, majorization-minimization, non-convexity, regularization.

*Both HS and GR were partially supported by NSF-DMS 1407028. GR was also partially supported by ARO W911NF-17-1-0357.

1 Introduction

In many classification problems, we are presented with the problem where it is either prohibitively expensive or impossible to obtain negative responses and we only have positive and unlabeled *presence-only* responses (see e.g. Ward et al. (2009)). For example, presence-only data is prevalent in geographic species distribution modeling in ecology where presences of species in specific locations are easily observed but absences are difficult to track (see e.g. Ward et al. (2009)), text mining (see e.g. Liu et al. (2003)), bioinformatics (see e.g. Elkan and Noto (2008)) and many other settings. Classification with presence-only data is sometimes referred to as PU-learning (see e.g. Liu et al. (2003); Elkan and Noto (2008)). In this paper we address the problem of variable selection with presence-only responses.

1.1 Motivating application: Biotechnology

Although the theory and methodology we develop apply generally, a concrete application that motivates this work arises from biological systems engineering. In particular, recent high-throughput technologies generate millions of biological sequences from a library for a protein or enzyme of interest (see e.g. Fowler and Fields (2014); Hietpas et al. (2011)). In Section 5 the enzyme of interest is beta-glucosidase (BGL) which is used to decompose disaccharides into glucose which is an important step in the process of converting plant matter to bio-fuels (Romero et al. (2015)). The performance of the BGL enzyme is measured by the concentration of glucose that is produced and a positive response arises when the disaccharide is decomposed to glucose and a negative response arises otherwise. Hence there are two scientific goals: firstly to determine how the sequence structure influences the biochemical functionality; secondly, using this relationship to engineer and design BGL sequences with improved functionality.

Given these two scientific goals, we are interested in both the *variable selection* and *classification* problem since we want to determine which positions in the sequence most

influence positive responses as well as classify which protein sequences are functional. Furthermore the number of variables here is large since we need to model long and complex biological sequences. Hence our variable selection problem is *high-dimensional*. In Section 5 we demonstrate the success of our algorithm in this application context.

1.2 Problem setup

To state the problem formally, let $x \in \mathbb{R}^p$ be a p -dimensional covariate such that $x \sim \mathbb{P}_X$, $y \in \{0, 1\}$ an associated response, and $z \in \{0, 1\}$ an associated label. If a sample is labeled ($z = 1$), its associated outcome is positive ($y = 1$). On the other hand, if a sample is unlabeled ($z = 0$), it is assumed to be randomly drawn from the population with only covariates x not the response y being observed. Given n_ℓ labeled and n_u unlabeled samples, the goal is to draw inferences about the relationship between y and x . We model the relationship between the probability of a response y being positive and (x, θ) using the standard logistic regression model:

$$\mathbb{P}(y = 1|x; \theta) = \frac{e^{\eta_\theta(x)}}{1 + e^{\eta_\theta(x)}}, \quad \eta_\theta(x) = \theta^T x \quad (1)$$

and $y|x \sim \mathbb{P}(\cdot|x; \theta^*)$ where $\theta^* \in \mathbb{R}^p$ refers to the unknown true parameter. Also, we assume the label z is assigned only based on the latent response y independent from x . Viewing z as a noisy observation of latent y , this assumption corresponds to a missing at random assumption, a classical assumption in latent variable problems.

Given such z , we select n_ℓ labeled and n_u unlabeled samples from samples with $z = 1$ and $z = 0$ respectively. An important issue is how positive and unlabeled samples are selected. In this paper we adopt a case-control approach (for example, McCullagh and Nelder (1989)) which is suitable for our biotechnology application and many others. In particular we introduce another binary random variable $s \in \{0, 1\}$ representing whether a sample is selected ($s = 1$) or not ($s = 0$) to model different sampling rates in selecting

labeled and unlabeled samples. Since there are n_ℓ labeled and n_u unlabeled samples, we have

$$\frac{\mathbb{P}(z = 1|s = 1)}{\mathbb{P}(z = 0|s = 1)} = \frac{n_\ell}{n_u},$$

and we see only selected samples, $(x_i, z_i, s_i = 1)_{i=1}^{n_\ell+n_u}$. It is further assumed that the selection is only based on the label z , independent of x and y . We note that this case-control scheme (Lancaster and Imbens (1996); Ward et al. (2009)), opposed to the single-training sampling scheme (Elkan and Noto (2008)) is needed to model the case where unlabeled samples are random draws from the original population, since positive samples have to be over-represented in the dataset to satisfy such model assumption.

In our biotechnology application the case-control setting is appropriate since the high-throughput technology leads to the unlabeled samples being drawn randomly from the original population (see Romero et al. (2015) for details). As is displayed in Fig. 1, sequences are selected randomly from a library and positive samples are generated through a screening step. Hence the positive sequences are sampled randomly from the positive sequences while the unlabeled sequences are based on random sampling from the original sequence library. This experiment corresponds exactly to the case-control sampling scheme discussed.

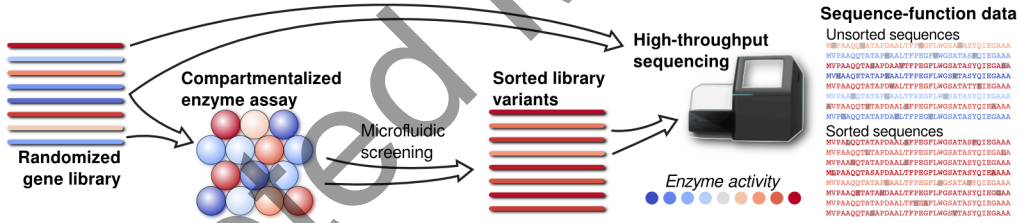


Figure 1: High-throughput sequencing diagram

Furthermore, the true positive prevalence is

$$\pi := \mathbb{P}(y = 1) = \int \frac{e^{\eta_{\theta^*}(x)}}{1 + e^{\eta_{\theta^*}(x)}} d\mathbb{P}_X(x) \in (0, 1) \quad (2)$$

and π is assumed known. In our biotechnology application, π is estimated precisely using an alternative experiment (Romero et al. (2015)).

In the biological sequence engineering example, $(x_i)_{i=1}^{n_\ell+n_u}$ correspond to binary covariates of biological sequences. In the BGL example, for each of the d positions, there are M possible categories of amino acids. Therefore the covariates correspond to the indicator of an amino acid appearing in a given position ($p = O(dM)$) as well as pairs of amino acids ($p = O(d^2M^2)$), and so on. Here $d = O(1000)$ and $M \approx 20$ make the problem high-dimensional.

High-dimensional PU-learning presents computational challenges since the standard logistic regression objective leads to a non-convex likelihood when we have positive and unlabeled data. To address this challenge, we build on the expectation-maximization (EM) procedure developed in Ward et al. (2009) and provide two computational speed-ups. In particular we introduce the *PULasso* for high-dimensional variable selection with positive and unlabeled data. Prior work that involves the EM algorithm in the low-dimensional setting in Ward et al. (2009) involves solving a logistic regression model at the M-step. To adapt to the high-dimensional setting and make the problem scalable, we include an ℓ_1 -sparsity or ℓ_1/ℓ_2 -group sparsity penalty and provide two speed-ups. Firstly we use a quadratic majorizer of the logistic regression objective, and secondly we use techniques in linear algebra to exploit sparsity of the design matrix X which commonly arises in the applications we are dealing with. Our PULasso algorithm fits into the majorization-minimization (MM) framework (see e.g. Lange et al. (2000); Ortega and Rheinboldt (2000)) for which the EM algorithm is a special case.

1.3 Our contributions

In this paper, we make the following major contributions:

- Develop the PULasso algorithm for doing variable selection and classification with

presence-only data. In particular we build on the existing EM algorithm developed in Ward et al. (2009) and add two computational speed-ups, quadratic majorization and exploiting sparse matrices. These two speed-ups improve speed by several orders of magnitude and allows our algorithm to scale to datasets with millions of samples and covariates.

- Provide theoretical guarantees for our algorithm. First we show that our algorithm converges to a stationary point of the non-convex objective, and then show that any stationary point within a local neighborhood of θ^* achieves the minimax optimal mean-squared error for sparse vectors. To provide statistical guarantees we extend the existing results of generalized linear model with a canonical link function (Negahban et al. (2012); Loh and Wainwright (2013)) to a non-canonical link function and show optimality of stationary points of non-convex objectives in high-dimensional statistics. To the best of our knowledge the PUlasso is the first algorithm where PU-learning is provably optimal in the high-dimensional setting.
- Demonstrate through a simulation study that our algorithm performs well in terms of classification compared to state-of-the-art PU-learning methods in Du Marthinus et al. (2015); Elkan and Noto (2008); Liu et al. (2003), both for low-dimensional and high-dimensional problems.
- Demonstrate that our PUlasso algorithm allows us to develop improved protein-engineering approaches. In particular we apply our PUlasso algorithm to sequences of BGL (beta-glucosidase) enzymes to determine which sequences are functional. We demonstrate that sequences selected by our algorithm have a good predictive accuracy and we also provide a scientific experiment which shows that the variables selected lead to BGL proteins that are engineered with improved functionality.

The remainder of the paper is organized as follows: in Section 2 we provide the back-

ground and introduce the PULasso algorithm, including our two computational speed-ups and provide an algorithmic guarantee that our algorithm converges to a stationary point; in Section 3 we provide statistical mean-squared error guarantees which show that our PULasso algorithm achieves the minimax rate; Section 4 provides a comparison in terms of classification performance of our PULasso algorithm to state-of-the-art PU-learning algorithms; finally in Section 5, we apply our PULasso algorithm to the BGL data application and provide both a statistical validation and simple scientific validation for our selected variables.

Notation: For scalars $a, b \in \mathbb{R}$, we denote $a \wedge b = \min\{a, b\}$, $a \vee b = \max\{a, b\}$. Also, we denote $a \gtrsim b$ if there exists a universal constant $c > 0$ such that $a \geq cb$. For $v, w \in \mathbb{R}^p$, we denote ℓ_1 , ℓ_2 , and ℓ_∞ norm as $\|v\|_1 = \sum_{i=1}^n |v_i|$, $\|v\|_2 = \sqrt{v^T v}$, and $\|v\|_\infty = \sup_j |v_j|$ and use $v \circ w \in \mathbb{R}^p$ to denote Hadamard product (entry-wise product) of v, w . For a set S , we use $|S|$ to denote the cardinality of S . For any subset $S \subseteq \{1, \dots, p\}$, $v_S \in \mathbb{R}^{|S|}$ denotes the sub-vector of the vector v by selecting the components with indices in S . Likewise for matrix $A \in \mathbb{R}^{n \times p}$, $A_S \in \mathbb{R}^{n \times |S|}$ denotes a sub-matrix by selecting columns with indices in S . For a group ℓ_1/ℓ_2 norm, the norm is characterized by a partition $\mathcal{G} := (g_1, \dots, g_J)$ of $\{1, \dots, p\}$ and associated weights $(w_j)_1^J$. We let $\mathcal{G} := (\mathcal{G}, (w_j)_1^J)$ and define the ℓ_1/ℓ_2 norm as $\|v\|_{\mathcal{G}, 2, 1} := \sum_j w_j \|v_{g_j}\|_2$. We often need a dual norm of $\|\cdot\|_{\mathcal{G}, 2, 1}$. We use $\bar{\mathcal{G}}$ to denote $\bar{\mathcal{G}} := (\mathcal{G}, (w_j^{-1})_1^J)$ and write $\|v\|_{\bar{\mathcal{G}}, 2, \infty} = \max_j w_j^{-1} \|v_{g_j}\|_2$. Finally we write $\mathbb{B}_q(r, v)$ for an ℓ_q ball with radius r centered at $v \in \mathbb{R}^p$, and denote as $\mathbb{B}_q(r)$ if $v = 0$.

For a convex function $f : \mathbb{R}^p \rightarrow \mathbb{R}$, we use $\partial f(x)$ to denote the set of sub-gradients at the point x and $\nabla f(x)$ to denote an element of $\partial f(x)$. Also for a function $f + g$ such that f is differentiable (but not necessarily convex) and g is convex, we define $\partial(f + g)(x) := \{\nabla f(x) + h \in \mathbb{R}^p; h \in \partial g(x)\}$ with a slight abuse of notation. Also, we say $f(n) = O(g(n))$, $f(n) = \Omega(g(n))$, and $f(n) = \Theta(g(n))$ if $|f|$ is asymptotically bounded above, bounded below, and bounded above and below by g .

For a random variable $x \in \mathbb{R}$, we say x is a sub-Gaussian random variable with sub-Gaussian parameter $\sigma_x > 0$ if $E[\exp(t(x - E[x]))] \leq \exp(t^2\sigma_x^2/2)$ for all $t \in \mathbb{R}$ and we denote as $x \sim \text{subG}(\sigma_x^2)$ with a slight abuse of notation. Similarly, we say x is a sub-exponential random variable with sub-exponential parameter (ν, b) if $E[\exp(t(x - E[x]))] \leq \exp(t^2\nu^2/2)$ for all $|t| \leq 1/b$ and we denote as $x \sim \text{subExp}(\nu, b)$. A collection of random variables (x_1, \dots, x_n) is referred to as x_1^n .

2 PUlasso algorithm

In this section, we introduce our PUlasso algorithm. First, we discuss the prior EM algorithm approach developed in Ward et al. (2009) and apply a simple regularization scheme. We then discuss our two computational speed-ups, the quadratic majorization for the M-step and exploiting sparse matrices. We prove that our algorithm has the descending property and converges to a stationary point, and show that our two speed-ups increase speed by several orders of magnitude.

2.1 Prior approach: EM algorithm with regularization

First we use the prior result in Ward et al. (2009) to determine the observed log-likelihood (in terms of the z_i 's) and the full log-likelihood (in terms of the unobserved y_i 's and z_i 's). The following lemma, derived in Ward et al. (2009), gives the form of the observed and the full log-likelihood in the case-control sampling scheme.

Lemma 2.1 (Ward et al. (2009)). *The observed log-likelihood $\log L(\theta; x_1^n, z_1^n)$ for our*

presence-only model in terms of $(x_i, z_i, s_i = 1)_{i=1}^n$ is:

$$\begin{aligned}\log L(\theta; x_1^n, z_1^n) &= \log \left(\prod_i \mathbb{P}_\theta(z_i | x_i, s_i = 1) \right) \\ &= \sum_{i=1}^n \log \left(\frac{\frac{n_l}{\pi n_u} e^{\theta^T x}}{1 + (1 + \frac{n_l}{\pi n_u}) e^{\theta^T x}} \right)^{z_i} \left(\frac{1 + e^{\theta^T x}}{1 + (1 + \frac{n_l}{\pi n_u}) e^{\theta^T x}} \right)^{1-z_i}\end{aligned}\quad (3)$$

The full log-likelihood $\log L_f(\theta; x_1^n, y_1^n, z_1^n)$ in terms of $(x_i, y_i, z_i, s_i = 1)_{i=1}^n$ is

$$\begin{aligned}\log L_f(\theta; x_1^n, y_1^n, z_1^n) &= \log \left(\prod_i \mathbb{P}_\theta(y_i, z_i | x_i, s_i = 1) \right) \\ &\propto \sum_{i=1}^n [y_i(x_i^T \theta + \log \frac{n_l + \pi n_u}{\pi n_u}) - \log(1 + \exp(x_i^T \theta + \log \frac{n_l + \pi n_u}{\pi n_u}))]\end{aligned}\quad (4)$$

where n_l, n_u are the number of positive and unlabeled observations, $n = n_l + n_u$ and π is defined in (2).

The proof can be found in Ward et al. (2009). Our goal is to estimate the parameter $\theta^* := \operatorname{argmin}_{\theta \in \mathbb{R}^p} E[-\log L(\theta; x_1^n, z_1^n)]$, which we assume to be unique. In the setting where p is large, we add a regularization term. We are interested in cases when there exists or does not exist a group structure within covariates. To be general we use the group ℓ_1/ℓ_2 -penalty for which ℓ_1 is a special case. Hence our overall optimization problem is:

$$\underset{\theta}{\text{minimize}} \quad -\frac{1}{n} \sum_{i=1}^n \log L(\theta; x_i, z_i) + P_\lambda(\theta) \quad (5)$$

where $\log L(\theta; x_i, z_i)$ is the observed log-likelihood. For a penalty term, we use the group sparsity regularizer

$$P_\lambda(\theta) := \lambda \|\theta\|_{\mathcal{G}, 2, 1} = \lambda \sum_{j=1}^J w_j \|\theta_{g_j}\|_2 \quad (6)$$

with $\mathcal{G} = (\mathcal{G}, (w_j)_{j=1}^J)$, such that $\mathcal{G} := (g_1, \dots, g_J)$ is a partition of $(1, \dots, p)$ and $w_j > 0$. We note that $\|\theta\|_{\mathcal{G}, 2, 1} = \|\theta\|_1$ if $J = p$, $g_j = \{j\}$ and $w_j = 1, \forall j$. For notational convenience we

denote the overall objective $\mathcal{F}_n(\theta)$ as

$$\mathcal{F}_n(\theta) := -\frac{1}{n} \sum_{i=1}^n \log L(\theta; x_i, z_i) + P_\lambda(\theta) = \mathcal{L}_n(\theta) + P_\lambda(\theta) \quad (7)$$

where we define the loss function $\mathcal{L}_n(\theta)$ as $\mathcal{L}_n(\theta) := -n^{-1} \sum_{i=1}^n \log L(\theta; x_i, z_i)$ and $P_\lambda(\theta) = \lambda \|\theta\|_{\mathcal{G}, 2, 1} = \lambda \sum_{j=1}^J w_j \|\theta_{g_j}\|_2$.

In the original proposal of the group lasso, Yuan and Lin (2006) recommended to use (6) for orthonormal group matrices X_{g_j} , i.e. $X_{g_j}^T X_{g_j} / n = I_{|g_j| \times |g_j|}$. If group matrices are not orthonormal however, it is unclear whether we should orthonormalize group matrices prior to application of the group lasso. This question was addressed in Simon and Tibshirani (2012), and the authors provide a compelling argument that prior orthonormalization has both theoretical and computational advantages. In particular, Simon and Tibshirani (2012) demonstrated that the following orthonormalization procedure is intimately connected with the uniformly most powerful invariant testing for inclusion of a group. To describe this orthonormalization explicitly, we obtain standardized group matrices $Q_{g_j} \in \mathbb{R}^{n \times |g_j|}$ and scale matrices $R_{g_j} \in \mathbb{R}^{|g_j| \times |g_j|}$ for $j \geq 2$ using the QR-decomposition such that

$$P_0 X_{g_j} = Q_{g_j} R_{g_j} \text{ and } Q_{g_j}^T Q_{g_j} = n I_{|g_j| \times |g_j|} \quad (8)$$

where $P_0 = (I_{n \times n} - \frac{1_n 1_n^T}{n})$ is the projection matrix onto the orthogonal space of 1_n . Letting $Q := [1_n, Q_{g_2}, \dots, Q_{g_J}] = [q_1^T, \dots, q_n^T]$, the original optimization problem (5) can be expressed in terms of q_i 's and becomes:

$$\underset{\nu}{\operatorname{argmin}} \left\{ -\frac{1}{n} \sum_{i=1}^n \log L(\nu; q_i, z_i) + \lambda \sum_{j=1}^J w_j \|\nu_{g_j}\|_2 \right\} \quad (9)$$

where we use the transformation θ to ν :

$$\theta_{g_j} = \begin{cases} \nu_1 - \sum_{j=2}^J \frac{1_n^T}{n} X_{g_j} R_{g_j}^{-1} \nu_{g_j} & j = 1 \\ R_{g_j}^{-1} \nu_{g_j} & j \geq 2. \end{cases} \quad (10)$$

We note that this corresponds to the standard centering and scaling of the predictors in the case of standard lasso. For more discussion about group lasso and standardization, see e.g. Huang et al. (2012).

A standard approach to performing this minimization is to use the EM-algorithm approach developed in Ward et al. (2009). In particular we treat y_1^n as hidden variables and estimate them in the E-step. Then use estimated \hat{y}_1^n to obtain the full log-likelihood $\log L_f(\theta; x_1^n, \hat{y}_1^n, z_1^n)$ in the M-step.

Algorithm 1: Regularized EM algorithm for the optimization problem (5)

1 Input: an initialization θ^0 such that $\mathcal{F}_n(\theta^0) \leq \mathcal{F}_n(\theta_{null})$

2 **for** $m=0, 1, 2, \dots$, **do**

• E-step : estimate y_i at $\theta = \theta^m$ by

$$\hat{y}_i(\theta^m) = \left(\frac{e^{x_i^T \theta^m}}{1 + e^{x_i^T \theta^m}} \right)^{1-z_i} \quad (11)$$

• M-step : obtain θ^{m+1} by

$$\theta^{m+1} \in \underset{\theta}{\operatorname{argmin}} \left\{ -\frac{1}{n} \sum_{i=1}^n \left(\hat{y}_i(\theta^m) (x_i^T \theta + b) - \log(1 + e^{x_i^T \theta + b}) \right) + P_\lambda(\theta) \right\} \quad (12)$$

$$\text{where } b := \log \frac{n_\ell + \pi n_u}{\pi n_u}$$

3 **end**

The E-step follows from $E_{\theta^m}[y_i | z_i, x_i, s_i = 1] = \left(\frac{e^{x_i^T \theta^m}}{1 + e^{x_i^T \theta^m}} \right)^{1-z_i}$ since $z_i = 1$ implies $y_i = 1$ and when $z_i = 0$, observations in the unlabeled data are random draws from the population. An initialization θ^0 can be any \mathbb{R}^p vector such that $\mathcal{F}_n(\theta^0) \leq \mathcal{F}_n(\theta_{null})$ where θ_{null} is the parameter corresponding to the intercept-only model. If we are provided with no additional information, we may use θ_{null} for the initialization. We use $\theta^0 = \theta_{null}$ as the initialization for the remainder of the paper. For the M-step it was originally proposed to use a logistic regression solver. We can use a regularized logistic regression solver such as

the **glmnet** R package to solve (12). We discuss a computationally more efficient way of solving (12) in the subsequent section.

2.2 PUlasso : A Quadratic Majorization for the M-step

Now we develop our PUlasso algorithm which is a faster algorithm for solving (5) by using quadratic majorization for the M-step. The main computational bottleneck in algorithm 1 is the M-step which requires minimizing a regularized logistic regression loss at each step. This sub-problem does not have a closed-form solution and needs to be solved iteratively, causing inefficiency in the algorithm. However the most important property of the objective function in the M-step is that it is a surrogate function of the likelihood which ensures the descending property (see e.g. Lange et al. (2000)). Hence we replace a logistic loss function with a computationally faster quadratic surrogate function. In this aspect, our approach is an example of the more general majorization-minimization (MM) framework (see e.g. Lange et al. (2000); Ortega and Rheinboldt (2000)).

On the other hand, our loss function itself belongs to a generalized linear model family, as we will discuss in more detail in the subsequent section. A number of works have developed methods for efficiently solving regularized generalized linear model problems. A standard approach is to make a quadratic approximation of the log-likelihood and use solvers for a regularized least-square problem. Works include using an exact Hessian (Lee et al. (2006); Friedman et al. (2010)), an approximate Hessian (Meier et al. (2008)) or a Hessian bound (Krishnapuram et al. (2005); Simon and Tibshirani (2012); Breheny and Huang (2013)) for the second order term. Solving a second-order approximation problem amounts to taking a Newton step, thus convergence is not guaranteed without a step-size optimization (Lee et al. (2006); Meier et al. (2008)), unless a global bound of the Hessian matrix is used. Our work can be viewed as in the line of these works where a quadratic approximation of the loss function is made and then an upper bound of the Hessian matrix

is used to preserve a majorization property.

A coordinate descent (CD) algorithm (Wu and Lange (2008); Friedman et al. (2010)) or a block coordinate descent (BCD) algorithm (Yuan and Lin (2006); Puig et al. (2011); Simon and Tibshirani (2012); Breheny and Huang (2013)) has been a very efficient and standard way to solve a quadratic problem with ℓ_1 penalty or ℓ_1/ℓ_2 penalty and we also take this approach. When a feature matrix $X \in \mathbb{R}^{n \times p}$ is sparse, we can set up the algorithm to exploit such sparsity through a sparse linear algebra calculation. We discuss this implementation strategy in the Section 2.2.1.

Now we discuss the PUlasso algorithm and the construction of quadratic surrogate functions in more details. Using the MM framework we construct the set of majorization functions $-\bar{Q}(\theta; \theta^m)$ with the following two properties:

$$\bar{Q}(\theta^m; \theta^m) = Q(\theta^m; \theta^m), \quad \bar{Q}(\theta; \theta^m) \leq Q(\theta; \theta^m), \forall \theta \quad (13)$$

where our goal is to minimize $-Q$ where $Q(\theta; \theta^m) := n^{-1} E_{\theta^m} [\log L_f(\theta) | z_1^n, x_1^n, s_1^n = 1]$.

Using the Taylor expansion of $Q(\theta; \theta^m)$ at $\theta = \theta^m$, we obtain $Q(\theta; \theta^m)$

$$\begin{aligned} &= Q(\theta^m; \theta^m) + \frac{1}{n} [X^T (\hat{y}(\theta^m) - \mu^*(\theta^m))]^T \Delta_m - \frac{1}{2n} \int_0^1 \Delta_m^T X^T W(\theta + s \Delta_m) X \Delta_m ds \\ &\geq Q(\theta^m; \theta^m) + \frac{1}{n} (\hat{y}(\theta^m) - \mu^*(\theta^m))^T X \Delta_m - \frac{1}{8n} \Delta_m^T X^T X \Delta_m \end{aligned}$$

where we define $\Delta_m := \theta - \theta^m$, $\mu^*(\theta^m)_i := \frac{e^{x_i^T \theta^m + b}}{1 + e^{x_i^T \theta^m + b}}$, $b := \log \frac{n_\ell + \pi n_u}{\pi n_u}$ and $W \in \mathbb{R}^{n \times n}$ is a diagonal matrix with $[W(\theta)]_{ii} := \mu^*(\theta)_i (1 - \mu^*(\theta)_i)$. The inequality follows from $W(\theta) \prec \frac{1}{4} I_{n \times n}$, $\forall \theta$. Thus setting \bar{Q} as follows:

$$\bar{Q}(\theta; \theta^m) := Q(\theta^m; \theta^m) + \frac{1}{n} (\hat{y}(\theta^m) - \mu^*(\theta^m))^T (X\theta - X\theta^m) - \frac{1}{8n} (\theta - \theta^m)^T X^T X (\theta - \theta^m),$$

\bar{Q} satisfies both conditions in (13). Also with some algebra, it follows that

$$\bar{Q}(\theta; \theta^m) = -\frac{1}{8n} (4(\hat{y}(\theta^m) - \mu^*(\theta^m)) + X\theta^m - X\theta)^T (4(\hat{y}(\theta^m) - \mu^*(\theta^m)) + X\theta^m - X\theta) + c(\theta^m)$$

for some $c(\theta^m)$ which does not depend on θ . Hence $-\bar{Q}$ acts as a quadratic surrogate function of $-Q$ which replaces our M-step for the original EM algorithm. Therefore our PULasso algorithm can be represented as follows.

Algorithm 2: PULasso : QM-EM algorithm for the optimization problem (5)

1 Input: an initialization θ^0 such that $\mathcal{F}_n(\theta^0) \leq \mathcal{F}_n(\theta_{null})$

2 for $m=0,1,2,\dots$, do

• E-step : estimate y_i at $\theta = \theta^m$ by

$$\hat{y}_i(\theta^m) = \left(\frac{e^{x_i^T \theta^m}}{1 + e^{x_i^T \theta^m}} \right)^{1-z_i} \quad (14)$$

• QM-EM step : obtain θ^{m+1} by

1. create a working response vector $u(\theta^m)$ at $\theta = \theta^m$

$$u(\theta^m) := 4(\hat{y}(\theta^m) - \mu^*(\theta^m)) + X\theta^m \quad (15)$$

2. solve a quadratic loss problem with a penalty

$$\theta^{m+1} \in \underset{\theta}{\operatorname{argmin}} \left\{ \frac{1}{2n} (u(\theta^m) - X\theta)^T (u(\theta^m) - X\theta) + 4P_\lambda(\theta) \right\} \quad (16)$$

3 end

Now we state the following proposition to show that both the regularized EM and PULasso algorithms have the desirable descending property and converge to a stationary point. For convenience we define the feasible region $\widetilde{\Theta}_0$, which contains all θ whose objective function value is better than that of the intercept-only model, defined as:

$$\widetilde{\Theta}_0 := \{\theta \in \mathbb{R}^p; \mathcal{F}_n(\theta) \leq \mathcal{F}_n(\theta_{null})\} \quad (17)$$

where $\theta_{null} = [\log \frac{\pi}{1-\pi}, 0, \dots, 0]^T$, an estimate corresponding to the intercept-only model.

We let \mathcal{S} be the set of stationary points satisfying the first order optimality condition, i.e.,

$$\mathcal{S} := \{\theta; \exists \nabla \mathcal{F}_n(\theta) \in \partial \mathcal{F}_n(\theta) \text{ such that } \nabla \mathcal{F}_n(\theta)^T (\theta' - \theta) \geq 0, \forall \theta' \in \widetilde{\Theta}_0\}. \quad (18)$$

One of the important conditions is to ensure that all iterates of our algorithm lie in $\widetilde{\Theta}_0$

which is trivially satisfied if $\theta^0 = \theta_{null}$.

Proposition 2.1. *The sequence of estimates (θ^m) obtained by Algorithms 1 or 2 satisfies*

- (i) $\mathcal{F}_n(\theta^m) \geq \mathcal{F}_n(\theta^{m+1})$, and $\mathcal{F}_n(\theta^m) > \mathcal{F}_n(\theta^{m+1})$ if $\theta^m \notin \mathcal{S}$.
- (ii) All limit points of $(\theta^m)_1^\infty$ are elements of the set \mathcal{S} , and $\mathcal{F}_n(\theta^m)$ converges monotonically to $\mathcal{F}_n(\tilde{\theta})$ for some $\tilde{\theta} \in \mathcal{S}$.
- (iii) The sequence (θ^m) has at least one limit point, which must be a stationary point of $\mathcal{F}_n(\theta)$ by (ii).

Proposition 2.1 shows that we obtain a stationary point of the objective (7) as an output of both the regularized EM algorithm and our PULasso algorithm. The proof uses the standard arguments based on Jensen's inequality, convergence of EM algorithm and MM algorithms and is deferred to the supplement S1.1.

2.2.1 Block Coordinate Descent Algorithm for M-step and Sparse Calculation

In this section, we discuss the specifics of finding a minimizer for the M-step (16) for each iteration of our PULasso algorithm. After pre-processing the design matrix as described in (9), (10), we solve the following optimization problem using a standard block-wise coordinate descent algorithm.

$$\underset{\nu}{\operatorname{argmin}} \left\{ \frac{1}{2n} \|u - Q\nu\|_2^2 + 4\lambda \sum_{j=1}^J w_j \|\nu_{g_j}\|_2 \right\} \quad (19)$$

Algorithm 3: Fitting (19) using Block Coordinate Descent

```

1 Given initial parameter  $\nu = [\nu_1, \nu_{g_2}^T \dots, \nu_{g_J}^T]^T$ , a residual vector  $r = u - \sum_{j=1}^J Q_{g_j} \nu_{g_j}$ 
2 for  $j=1$  do
3   | update  $\nu_1$  and  $r$  using (20)-(22)
4 end
5 repeat
6   | for  $j=2, \dots, J$  do
7     |
7     |  $z_j = n^{-1} Q_{g_j}^T r + \nu_{g_j}$  (20)
7     |  $\nu'_{g_j} \leftarrow S(z_j, 4\lambda w_j)$  (21)
7     |  $r' \leftarrow r + Q_{g_j}(\nu_{g_j} - \nu'_{g_j})$  (22)
7     |  $r \leftarrow r', \nu_{g_j} \leftarrow \nu'_{g_j}$ 
8   | end
9 until convergence;

```

$S(., \lambda)$ is the soft thresholding operator defined as follows:

$$S(z, \lambda) := \begin{cases} (\|z\|_2 - \lambda) \frac{z}{\|z\|_2} & \text{if } \|z\|_2 > \lambda \\ 0 & \text{otherwise.} \end{cases}$$

Note that we do not need to keep updating the intercept ν_1 since $Q_{g_j}, j \geq 2$ are orthogonal to $Q_{g_1} \equiv \mathbb{1}_n$. For more details, see e.g. Breheny and Huang (2013).

For our biochemistry example and many other examples, X is a sparse matrix since each entry is an indicator of whether an amino acid is in a position. In Algorithm 3, we do not exploit this sparsity since Q will not be sparse even when X is sparse. If we want to exploit sparse X we use the following algorithm.

Algorithm 4: Fitting (19) and exploiting sparse X

```

1 Given initial parameter  $\nu = [\nu_1, \nu_{g_2}^T \dots, \nu_{g_J}^T]^T$ ,  $r = u - P_0(\sum_{j=1}^J X_{g_j} R_{g_j}^{-1} \nu_{g_j})$ 
2 for  $j=1$  do
3   | update  $\nu_1$  and  $r$  using (20)-(22).
4 end
5 repeat
6   for  $j=2, \dots, J$  do
7     |
7        $z_j = n^{-1} R_{g_j}^{-1} X_{g_j}^T r - R_{g_j}^{-1} (X_{g_j}^T \mathbb{1}_n / n) (\mathbb{1}_n^T r / n) + \nu_{g_j}$  (23)
7        $\nu'_{g_j} \leftarrow S(z_j, 4\lambda w_j)$  (24)
7        $r' \leftarrow r + X_{g_j} R_{g_j}^{-1} (\nu_{g_j} - \nu'_{g_j})$  (25)
7        $a_j \leftarrow \mathbb{1}_n^T X_{g_j} R_{g_j}^{-1} (\nu_{g_j} - \nu'_{g_j}) / n$  (26)
7        $r \leftarrow r', \nu_{g_j} \leftarrow \nu'_{g_j}$ 
8   end
9
9        $r \leftarrow r - (\sum_{j=2}^J a_j) \mathbb{1}_n$  (27)
10 until convergence;

```

To explain the changes to this algorithm, we modify (20) and (22) so that we directly use X rather than Q to exploit the sparsity of X . Using (8), we first substitute Q_{g_j} with $P_0 X_{g_j} R_{g_j}^{-1}$ to obtain

$$z_j = n^{-1} R_{g_j}^{-1} X_{g_j}^T P_0 r + \nu_{g_j} \quad (28)$$

$$r' \leftarrow r + P_0 X_{g_j} R_{g_j}^{-1} (\nu_{g_j} - \nu'_{g_j}). \quad (29)$$

However carrying out (28)-(29) instead of (20)-(22) incurs a greater computational cost. Calculating $Q_{g_j}^T r$ requires $n|g_j|$ operations. On the contrary, the minimal number of operations required to do a matrix multiplication of $R_{g_j}^{-1} X_{g_j}^T P_0 r$ is $n^2 + n|g_j| + |g_j|^2$, when it is parenthesized as $R_{g_j}^{-1} (X_{g_j}^T (P_0 r))$. In many cases $|g_j|$ is small (for standard lasso, $|g_j| = 1, \forall j$ and for our biochemistry example, $|g_j|$ is at most 20), but the additional increase in n can

be very costly (especially in our example where n is over 4 million).

For a more efficient calculation, we first exploit the structure of $P_0 = I_{n \times n} - \frac{1_n 1_n^T}{n}$ when multiplying P_0 with a vector, which reduces the cost from n^2 operations to $2n$ operations. Also, we carry out calculations using X_{g_j} instead of $P_0 X_{g_j}$ when calculating residuals and do the corrections all at once.

Before going into detail about (23)-(26), we first discuss the computational complexity. Comparing (23) with (20), the first term only requires an additional $|g_j|^2$ operations. The second term $(X_{g_j}^T 1_n)/n$ can be stored during the initial QR decomposition; thus the only potentially expensive operation is calculating an average of r which requires n operations. Comparing (25) with (22), only $|g_j|^2$ additional operations are needed when we parenthesize as $X_{g_j}(R_{g_j}^{-1}(\nu_{g_j} - \nu'_{g_j}))$. Note that if we had kept P_0 , there would have been an additional $2n$ operations even though we had used the structure of P_0 . In the calculation of (27), we note that n operations are involved in subtracting $\sum_{j=2}^J a_j$ from r because a_j are scalars. In summary, we essentially reduce additional computational cost from $O(n^2)$ to nJ per cycle by carrying out (23)-(26) instead of (28)-(29).

Now we derive/explain the formulas in Algorithm 4. To make quantities more explicit, we use r_j and r'_j to denote a residual vector before/after update at j using Algorithm 3 and \tilde{r}_j and \tilde{r}'_j using Algorithm 4. By definition, $r_{j+1} = r'_j$ and $\tilde{r}_{j+1} = \tilde{r}'_j$. Also we note that in the beginning of the cycle $r_2 = \tilde{r}_2$. Equation (23) can be obtained from (28) by replacing P_0 with $I_{n \times n} - \frac{1_n 1_n^T}{n}$. Now we show that modified residuals still correctly update coefficients. Starting from $j = 2$, a calculated residual \tilde{r}'_j is a constant vector off from a correct residual r'_j , as we see below:

$$r'_j = r_j + P_0 X_{g_j} R_{g_j}^{-1}(\nu_{g_j} - \nu'_{g_j}) \quad (30)$$

$$= r_j + X_{g_j} R_{g_j}^{-1}(\nu_{g_j} - \nu'_{g_j}) - 1_n \frac{1_n^T}{n} X_{g_j} R_{g_j}^{-1}(\nu_{g_j} - \nu'_{g_j}) \quad (31)$$

$$= \tilde{r}'_j - 1_n a_j \quad (32)$$

where we recall that $a_j = \frac{1}{n} X_{g_j}^T R_{g_j}^{-1} (\nu_{g_j} - \nu'_{g_j})$. We note $P_0 r'_j = P_0 \tilde{r}'_j$ because $P_0 \mathbb{1}_n = 0$. Then the next z_{j+1} , thus new $\nu_{g_{j+1}}$, are still correctly calculated since

$$z_{j+1} = n^{-1} R_{g_{j+1}}^{-1} X_{g_{j+1}}^T P_0 r_{j+1} + \nu_{g_{j+1}} = n^{-1} R_{g_{j+1}}^{-1} X_{g_{j+1}}^T P_0 \tilde{r}_{j+1} + \nu_{g_{j+1}}. \quad (33)$$

The next residual \tilde{r}'_{j+1} is again off by a constant from the correct residual r'_{j+1} . To see this, $r'_{j+1} = r_{j+1} + P_0 X_{g_{j+1}} R_{g_{j+1}}^{-1} (\nu_{g_{j+1}} - \nu'_{g_{j+1}}) = \tilde{r}_{j+1} + P_0 X_{g_{j+1}} R_{g_{j+1}}^{-1} (\nu_{g_{j+1}} - \nu'_{g_{j+1}}) - a_j \mathbb{1}_n$ by (29). Going through (30)-(32) with j being replaced by $j+1$, we obtain

$$r'_{j+1} = \tilde{r}'_{j+1} - (a_j + a_{j+1}) \mathbb{1}_n.$$

Inductively, we have correct z_j , thus ν_{g_j} for all $j \geq 2$. At the end of the cycle, we correct the residual vector all at once by letting $r \leftarrow r - (\sum_{j=2}^J a_j) \mathbb{1}_n$.

2.3 R Package details

We provide a publicly available R implementation of our algorithm in the **PUlasso** package. For a fast and efficient implementation, all underlying computation is implemented in C++. The package uses warm start and strong rule (Friedman et al. (2007); Tibshirani et al. (2012)), and a cross-validation function is provided as well for the selection of the regularization parameter λ . Our package supports a parallel computation through the R package **parallel**.

2.4 Run-time improvement

Now we illustrate the run-time improvements for our two speed-ups. Note that we only include p up to 100 so that we can compare to the original regularized EM algorithm. For our biochemistry application $p = O(10^4)$ and $n = O(10^6)$ which means the regularized EM algorithm is too slow to run efficiently. Hence we use smaller values of n and p in our run-time comparison. It is clear from our results that the quadratic majorization step is several

orders of magnitude faster than the original EM algorithm, and exploiting the sparsity of X provides a further 30% speed-up.

	(n,p)	PULasso	EM	time reduction(%)
Dense matrix	n=1000, p=10	0.94	443.72	99.79
	n=5000, p=50	2.52	1844.98	99.86
	n=10000, p=100	9.45	5066.86	99.81
Sparse matrix	n=1000, p=10	0.40	196.86	99.80
	n=5000, p=50	2.01	614.65	99.67
	n=10000, p=100	4.29	1201.09	99.64

Table 1: Timings (in seconds). Sparsity level in $X = 0.95$, $n_\ell/n_u = 0.5$. Total time for 100 λ values, averaged over 3 runs.

(n,p)	sparse calculation	dense calculation	time reduction(%)
n=10000, p=100	12.91	19.24	32.89
n=30000, p=100	25.64	38.73	33.79
n=50000, p=100	39.47	57.18	30.97

Table 2: Timings (in seconds) using sparse and dense calculation for fitting the same simulated data. Sparsity level in $X = 0.95$, $n_\ell/n_u = 0.5$. Total time for 100 λ values, averaged over 3 runs.

3 Statistical Guarantee

We now turn our attention to statistical guarantees for our PULasso algorithm under the statistical model (1). In particular we provide error bounds for any stationary point of the non-convex optimization problem (5). Proposition 2.1 guarantees that we obtain a stationary point from our PULasso algorithm.

We first note that the observed likelihood (3) is a generalized linear model (GLM) with a non-canonical link function. To see this, we rewrite the observed likelihood (3) as

$$L(\theta; x_1^n, z_1^n) = \prod_{i=1}^n \exp(z_i \eta_i - A(\eta_i)) \quad (34)$$

after some algebraic manipulations, where we define $\eta_i := \log(n_\ell/\pi n_u) + x_i^T \theta - \log(1 + e^{x_i^T \theta})$ and $A(\eta_i) := \log(1 + e^{\eta_i})$. Also, we let $\mu(\eta_i) := A'(\eta_i)$, which is the conditional mean of z_i given x_i , by the property of exponential families. For the convenience of the reader, we include the derivation from (3) to (34) in the supplementary material S2.1. The mean of z_i is related with $\theta^T x_i$ via the link function g through $g(\mu(\eta_i)) = \theta^T x_i$, where g satisfies $(g \circ \mu)^{-1}(\theta^T x_i) = \log(n_\ell/\pi n_u) + x_i^T \theta - \log(1 + e^{x_i^T \theta})$. Because $(g \circ \mu)^{-1}$ is not the identity function, the likelihood is not convex anymore. For a more detailed discussion about the GLM with non-canonical link, see e.g. McCullagh and Nelder (1989); Fahrmeir and Kaufmann (1985).

A number of works have been devoted to sparse estimation for generalized linear models. A large number of previous works have focused on generalized linear models with convex loss functions (negative log-likelihood with a canonical link) plus ℓ_1 or ℓ_1/ℓ_2 penalties. Results with the ℓ_1 penalty include a risk consistency result (van de Geer (2008)) and estimation consistency in ℓ_2 or ℓ_1 norms (Kakade et al. (2010)). For a group-structured penalty, a probabilistic bound for the prediction error was given in Meier et al. (2008). An ℓ_2 estimation error bound in the case of the group lasso was given in Blazre et al. (2014).

Negahban et al. (2012) re-derived an ℓ_2 error bound of an ℓ_1 -penalized GLM estimator under the unified framework for M-estimators with a convex loss function. This result about the regularized GLM was generalized in Loh and Wainwright (2013) where penalty functions are allowed to be non-convex, while the same convex loss function was used. Since the overall objective function is non-convex, authors discuss error bounds obtained for any stationary point, not a global minimum. In this aspect, our work closely follows this idea.

However, our setting differs from Loh and Wainwright (2013) in two aspects: first, the loss function in our setting is non-convex, in contrast with a convex loss function (a negative log-likelihood with a canonical link) with non-convex regularizer in Loh and Wainwright (2013). Also, an additive penalty function was used in the work of Loh and Wainwright (2013), but we consider a group-structured penalty.

After the initial draft of this paper was written, we became aware of two recent papers (Elsener and van de Geer (2018); Mei et al. (2018)) which studied non-convex M-estimation problems in various settings including binary linear classification, where the goal is to learn θ^* such that $E[z_i|x_i] = \sigma(x_i^T \theta^*)$ for a known $\sigma(\cdot)$. The proposed estimators are stationary points of the optimization problem: $\arg\min_{\theta} n^{-1} \sum_{i=1}^n (z_i - \sigma(x_i^T \theta))^2 + \lambda \|\theta\|_1$ in both papers. As the focus of our paper is to learn a model with a structural contamination in responses, our choice of mean and loss functions differ from both papers. In particular, our choice of mean function is different from the sigmoid function, which was the representative example of $\sigma(\cdot)$ in both papers, and we use the negative log-likelihood loss in contrast to the squared loss. We establish error bounds by proving a modified restricted strong convexity condition, which will be discussed shortly, while error bounds of the same rates were established in Elsener and van de Geer (2018) through a sharp oracle inequality, and a uniform convergence result over population risk in Mei et al. (2018).

Due to the non-convexity in the observed log-likelihood, we limit the feasible region Θ_0 to

$$\Theta_0 := \{\theta \in \mathbb{R}^p; \|\theta\|_2 \leq r_0, \|\theta\|_{\mathcal{G},2,1} \leq R_n\} \quad (35)$$

for theoretical convenience. Here $r_0, R_n > 0$ must be chosen appropriately and we discuss these choices later. Similar restriction is also assumed in Loh and Wainwright (2013).

3.1 Assumptions

We impose the following assumptions. First, we define a sub-Gaussian tail condition for a random vector $x \in \mathbb{R}^p$; we say x has a sub-Gaussian tail with parameter σ_x^2 , if for any fixed $v \in \mathbb{R}^p$, there exists $\sigma_x > 0$ such that $E[\exp(t(x - E[x])^T v)] \leq \exp(t^2 \|v\|_2^2 \sigma_x^2 / 2)$ for any $t \in \mathbb{R}$. We recall that θ^* is the true parameter vector, which minimizes the population loss.

Assumption 1. *The rows $x_i \in \mathbb{R}^p$, $i = 1, 2, \dots, n$ of the design matrix are i.i.d. samples from a mean-zero distribution with sub-Gaussian tails with parameter σ_x^2 . Moreover, $\Sigma_x := E[x_i x_i^T]$ is a positive definite and with minimum eigenvalue $\lambda_{\min}(\Sigma_x) \geq K_0$ where K_0 is a constant bounded away from 0. We further assume that $(x_{ij})_{j \in g_j}$ are independent for all $j \in g_j$ and $g_j \in \mathcal{G}$.*

Similar assumptions appear in for e.g. Negahban et al. (2012). This restricted minimum eigenvalue condition (see e.g. Raskutti et al. (2010) for details) is satisfied for weakly correlated design matrices. We further assume independence across covariates *within groups* since sub-Gaussian concentration bound assuming independence within groups is required.

Assumption 2. *For any $r > 0$, there exists K_1^r such that $\max_i |x_i^T \theta| \leq K_1^r$ a.s. for all θ in the set $\{\theta : \|\theta - \theta^*\|_2 \leq r \cap \text{supp}(\theta - \theta^*) \subseteq g_j \text{ for some } g_j \in \mathcal{G}\}$.*

Assumption 2 ensures that $|x_i^T \theta^*|$ is bounded a.s., which guarantees that the underlying probability $(1 + e^{-x_i^T \theta^*})^{-1}$ is between 0 and 1, and $|x_i^T \theta|$ is also bounded within a compact sparse neighborhood of θ^* which ensures concentration to the population loss. Comparable assumptions are made in Elsener and van de Geer (2018); Mei et al. (2018) where similar non-convex M estimation problems are investigated.

Assumption 3. *The ratio of the number of labeled to unlabeled data, i.e. n_ℓ/n_u is lower bounded away from 0 and upper bounded for all $n = n_\ell + n_u$, as $n \rightarrow \infty$. Equivalently, there is a constant K_2 such that $|\log(n_\ell/\pi n_u)| \leq K_2$*

Assumption 3 ensures that the number of labeled samples n_ℓ is not too small or large relative to n . The reason why n_ℓ can not be too large is that the labeled samples are only positives and we need a reasonable number of negative samples which are a part of the unlabeled samples.

Assumption 4 (Rate conditions). *We assume a high-dimensional regime where both $(n, p) \rightarrow \infty$ and $\log p = o(n)$. For $\mathcal{G} = ((g_1, \dots, g_J), (w_j)_1^J)$ and $m := \max_j |g_j|$, we assume $J = \Omega(n^\beta)$ for some $\beta > 0$, $m = o(n \wedge J)$, $\min_j w_j = \Omega(1)$, and $\max_j w_j = o(n \wedge J)$.*

Assumption 4 states standard rate conditions in a high-dimensional setting. In terms of the group structure, we assume that growth of p is not totally attributed to the expansion of a few groups; the number of groups J increases with n , and the maximum group size m is of small order of both n and J . Also we note that a typical choice of $w_j = \sqrt{|g_j|}$ satisfies Assumption 4 because $\min_j w_j \geq 1$, $\max_j w_j = \sqrt{m}$ and $\sqrt{m}/n, \sqrt{m}/J = o(1)$.

Finally we define the restricted strong convexity assumption for a loss function following the definition in Loh and Wainwright (2013).

Definition 3.1 (Restricted strong convexity). *We say \mathcal{L}_n satisfies a restricted strong convexity (RSC) condition with respect to θ^* with curvature $\alpha > 0$ and tolerance function τ over Θ_0 if the following inequality is satisfied for all $\theta \in \Theta_0$:*

$$(\nabla \mathcal{L}_n(\theta) - \nabla \mathcal{L}_n(\theta^*))^T \Delta \geq \alpha \|\Delta\|_2^2 - \tau(\|\Delta\|_{\mathcal{G}, 2, 1}) \quad (36)$$

where $\Delta := \theta - \theta^*$ and $\tau(\|\Delta\|_{\mathcal{G}, 2, 1}) = \tau_1 \|\Delta\|_{\mathcal{G}, 2, 1}^2 \frac{\log J + m}{n} + \tau_2 \|\Delta\|_{\mathcal{G}, 2, 1} \sqrt{\frac{\log J + m}{n}}$.

In the special case where $\|\Delta\|_{\mathcal{G}, 2, 1} = \|\Delta\|_1$ and hence $\tau(\|\Delta\|_1) = \tau_1 \|\Delta\|_1^2 \frac{\log p}{n} + \tau_2 \|\Delta\|_1 \sqrt{\frac{\log p}{n}}$, similar RSC conditions were discussed in Negahban et al. (2012) and Loh and Wainwright (2013) with different τ and Θ_0 . One of the important steps in our proof is to prove that RSC holds for the objective function $\mathcal{L}_n(\theta)$.

3.2 Guarantee

Under Assumptions 1-4, we will show in Theorem 3.2 that the RSC condition holds with high probability over $\{\theta; \|\theta\|_2 \leq r_0\}$ and therefore over Θ_0 , for Θ_0 defined in (35). Under the RSC assumption, the following proposition, which is a modification of Theorem 1 in Loh and Wainwright (2013), provides ℓ_1/ℓ_2 and ℓ_2 bounds of an error vector $\hat{\Delta} := \hat{\theta} - \theta^*$. Recall that $m = \max_j |g_j|$ (the size of the largest group) and J is the number of groups.

Proposition 3.1. *Suppose the empirical loss \mathcal{L}_n satisfies the RSC condition (36) with $\tau(\|\Delta\|_{\mathfrak{g},2,1}) = \tau_1 \|\Delta\|_{\mathfrak{g},2,1}^2 \frac{\log J + m}{n} + \tau_2 \|\Delta\|_{\mathfrak{g},2,1} \sqrt{\frac{\log J + m}{n}}$ over Θ_0 where Θ_0 is feasible region for the objective (5), as defined in (35), and the true parameter vector θ^* is feasible, i.e. $\theta^* \in \Theta_0$. Consider λ such that*

$$4 \max \left\{ \|\nabla \mathcal{L}_n(\theta^*)\|_{\mathfrak{g},2,\infty}, \left(\tau_1 \frac{2R_n(\log J + m)}{n} + \tau_2 \sqrt{\frac{(\log J + m)}{n}} \right) \right\} \leq \lambda. \quad (37)$$

Let $\hat{\theta}$ be a stationary point of (5). Then the following error bounds

$$\|\hat{\Delta}\|_2 \leq (\max_{j \in S} w_j) \frac{3\sqrt{s}\lambda}{2\alpha} \quad \text{and} \quad \|\hat{\Delta}\|_{\mathfrak{g},1,2} \leq (\max_{j \in S} w_j)^2 \frac{6s\lambda}{\alpha}, \quad (38)$$

hold where $S := \{j \in (1, \dots, J); \theta_{g_j}^* \neq 0\}$ and $s := |S|$.

The proof for Proposition 3.1 is deferred to the supplementary material S2.3. From (38), we note the squared ℓ_2 -error to grow proportionally with s and λ^2 . If $\theta^* \in \Theta_0$ and the choice of $\lambda = \Theta \left(\sqrt{\frac{\log J + m}{n}} \right)$ satisfies the inequality (37), we obtain squared ℓ_2 error which scales as $s \frac{\log J + m}{n}$, provided that the RSC condition holds over Θ_0 . In the case of lasso we recover $\frac{s \log p}{n}$ parametric optimal rate since $J = p, m = 1$.

With the choice of $r_0 \geq \|\theta^*\|_2$ and $R_n = \Theta \left(\sqrt{\frac{n}{\log J + m}} \right)^1$, we ensure θ^* is feasi-

¹We note that the group ℓ_1 constraint is active only if $\sqrt{\frac{n}{\log J + m}} = \mathcal{O}((\max_j w_j)r_0\sqrt{J})$. If $R_n \geq (\max_j w_j)r_0\sqrt{J}$, $\Theta_0 = \{\theta; \|\theta\|_2 \leq r_0, \|\theta\|_{\mathfrak{g},2,1} \leq R_n\} \supseteq \{\theta; \|\theta\|_2 \leq r_0, \|\theta\|_{\mathfrak{g},2,1} \leq (\max_j w_j)r_0\sqrt{J}\} \supseteq \{\theta; \|\theta\|_2 \leq r_0\}$ by the ℓ_1 - ℓ_2 inequality, i.e. if $\|\theta\|_2 \leq r_0$, $\|\theta\|_{\mathfrak{g},2,1} \leq (\max_j w_j)r_0\sqrt{J}$. The other direction is trivial, and thus Θ_0 is reduced to $\Theta_0 = \{\theta; \|\theta\|_2 \leq r_0\}$.

ble and $\lambda = \Theta\left(\sqrt{\frac{\log J+m}{n}}\right)$ satisfies the inequality (37) with high probability. Clearly $\left(\tau_1 \frac{2R_n(\log J+m)}{n} + \tau_2 \sqrt{\frac{\log J+m}{n}}\right)$ is of the order $\sqrt{\frac{\log J+m}{n}}$ with the choice of $R_n = \Theta\left(\sqrt{\frac{n}{\log J+m}}\right)$, and following Lemma 3.1, we have $\|\nabla \mathcal{L}_n(\theta^*)\|_{\tilde{\mathcal{G}},2,\infty} = \mathcal{O}\left(\sqrt{\frac{\log J+m}{n}}\right)$ with high probability. Thus inequality (37) is satisfied with $\lambda = \Theta\left(\sqrt{\frac{\log J+m}{n}}\right)$ w.h.p. as well.

Lemma 3.1. *Under Assumptions 1-4, for any given $\epsilon > 0$, there is a positive constant c such that*

$$\mathbb{P}\left(\|\nabla \mathcal{L}_n(\theta^*)\|_{\tilde{\mathcal{G}},2,\infty} \geq c\sqrt{\frac{\log J+m}{n}}\right) \leq \epsilon$$

given a sample size $n \gtrsim (\log p + m) \vee (1/\epsilon)^{1/\beta}$.

The proof for Lemma 3.1 is provided in the supplement S2.4. Now we state the main theorem of this section which shows that RSC condition holds uniformly over a neighborhood of the true parameter.

Theorem 3.2. *For any given $r > 0$ and $\epsilon > 0$, there exist strictly positive constants α, τ_1 and τ_2 depending on σ_x, K_0, K_1^r and K_2 such that*

$$(\nabla \mathcal{L}_n(\theta) - \nabla \mathcal{L}_n(\theta^*))^T \Delta \geq \alpha \|\Delta\|_2^2 - \tau_1 \|\Delta\|_{\mathcal{G},2,1}^2 \frac{\log J+m}{n} - \tau_2 \|\Delta\|_{\mathcal{G},2,1} \sqrt{\frac{\log J+m}{n}} \quad (39)$$

holds for all θ such that $\|\Delta\|_2 := \|\theta - \theta^*\|_2 \leq r$ with probability at least $1 - \epsilon$, given (n, p) satisfying $n \gtrsim (\log J + m) \vee (1/\epsilon)^{1/\beta}$.

The proof of Theorem 3.2 is deferred to the supplement S2.5. There are a couple of notable remarks about Theorem 3.2 and Proposition 3.1.

- The application of the Proposition 3.1 requires for a RSC condition to hold over a feasible region Θ_0 . Setting $r = 2r_0$ in Theorem 3.2, inequality (39) holds over $\{\theta; \|\theta - \theta^*\|_2 \leq 2r_0\}$ w.h.p, therefore over $\Theta_0 \subseteq \{\theta; \|\theta - \theta^*\|_2 \leq 2r_0\}$.

- We discuss how underlying parameters r_0, σ_x , and constants K_0 - K_2 in Assumptions 1-3 are related to the ℓ_2 -error bound. From Proposition 3.1, we see that ℓ_2 -error is proportional to τ_1/α and τ_2/α . The proof of Theorem 3.2 reveals that $\tau_1/\alpha \lesssim (\sigma_x K_3/K_0)^2$ and $\tau_2/\alpha \lesssim \sigma_x(1 + K_1^{2r_0})/K_0 L_0$, where L_0 and K_3 are also constants defined as $L_0 := \inf_{|u| \leq K_2 + K_1^{2r_0} + 2r_0 K_3} (e^u/(1 + e^u)^2)(1 + e^{K_1^{2r_0} + 2r_0 K_3})^{-2}$ and $K_3 \lesssim \sigma_x \log(\sigma_x^2/K_0)^{1/2}$. As L_0 is inversely related to K_2 and r_0 , ℓ_2 -error is proportional to the r_0 , σ_x , $K_1^{2r_0}$ and K_2 in Assumptions 2 and 3, but inversely related to the minimum eigenvalue bound K_0 in Assumption 1.
- The mean-squared error $\frac{s \log p}{n}$ in the case of $J = p$ is verified below in Fig. 2 and both the mean-squared error and ℓ_1 errors are minimax optimal for high-dimensional linear regression (Raskutti et al. (2011)).

To validate the mean-squared error upper bound of $\frac{s \log p}{n}$ in Section 3, a synthetic dataset was generated according to the logistic model (1) with $p = 500$ covariates and $X \sim N(0, I_{500 \times 500})$. Varying s and n were considered to study the rate of convergence of $\|\hat{\theta} - \theta^*\|_2$. The ratio n_ℓ/n_u was fixed to be 1. For each dataset, $\hat{\theta}$ was obtained by applying PULasso algorithm with a lambda sequence $\lambda_n := c_s \sqrt{\frac{\log p}{n}}$ for a suitably chosen c_s for each s . We repeated the experiment 100 times and average ℓ_2 -error was calculated. In Figure 2, we illustrate the rate of convergence of $\|\hat{\theta} - \theta^*\|_2$. In particular, $\|\hat{\theta} - \theta^*\|_2$ against $\sqrt{\frac{s \log p}{n}}$ is plotted with varying s and n . The error appears to be linear in $\sqrt{\frac{s \log p}{n}}$, and thus we also empirically conclude that our algorithm achieves the optimal $\sqrt{\frac{s \log p}{n}}$ rate.

4 Simulation study: Classification performance

In this section, we provide a simulation study which validates the classification performance for PULasso. In particular we provide a comparison in terms of classification performance to state-of-the-art methods developed in Du Marthinus et al. (2015); Elkan and Noto (2008);

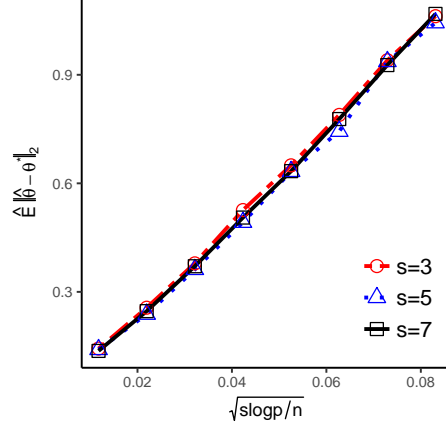


Figure 2: $\hat{E}[\|\hat{\theta} - \theta\|_2^2]$ plotted against $\sqrt{s \log p / n}$ with fixed $p=500$ and varying s and n

Liu et al. (2003). The focus of this section is classification rather than variable selection since many of the state-of-the-art methods we compare to are developed mainly for classification and are not developed for variable selection.

4.1 Comparison methods

Our experiments compare six algorithms: (i) logistic regression model assuming we know the true responses (*oracle* estimator); (ii) our PULasso algorithm; (iii) a bias-corrected logistic regression algorithm in Elkan and Noto (2008); (iv) a second algorithm from Elkan and Noto (2008) that is effectively a one-step EM algorithm; (v) the biased SVM algorithm from Liu et al. (2003) and (vi) the PU-classification algorithm based on an asymmetric loss from Du Marthinus et al. (2015).

The biased SVM from Liu et al. (2003) is based on the supported vector machine (SVM) classifier with two tuning parameters which parameterize mis-classification costs of each kind. The first algorithm from Elkan and Noto (2008) estimates label probabilities $\mathbb{P}(z = 1|x)$ and corrects the bias in the classifier via the estimation of $\mathbb{P}(z = 1|y = 1)$ under the

assumption of a disjoint support between $\mathbb{P}(x|y = 1)$ and $\mathbb{P}(x|y = 0)$. Their second method is a modification of the first method; a unit weight is assigned to each labeled sample, and each unlabeled example is treated as a combination of a positive and negative example with weight $\mathbb{P}(y = 1|x, z = 0)$ and $\mathbb{P}(y = 0|x, z = 0)$, respectively. Du Marthinus et al. (2015) suggests using asymmetric loss functions with ℓ_2 -penalty. Asymmetric loss function is considered to cancel the bias induced by separating positive and unlabeled samples rather than positive and negative samples. Any convex surrogate of 0-1 loss function can be used for the algorithm. There is a publicly available matlab implementation of the algorithm when a surrogate is the squared loss on the author's webpage² and since we use their code and implementation, the squared loss is considered.

4.2 Setup

We consider a number of different simulation settings: (i) small and large p to distinguish the low and high-dimensional setting; (ii) weakly and strongly separated populations; (iii) weakly and highly correlated features; and (iv) correctly specified (logistic) or mis-specified model. Given dimensions (n, p) , sparsity level s , predictor auto-correlation ρ , separation distance d , and model specification scheme (logistic, mis-specified), our setup is the following:

- Choose the active covariate set $S \subseteq \{1, 2, \dots, p\}$ by taking s elements uniformly at random from $(1, 2, \dots, p)$. We let true $\theta^* \in \mathbb{R}^p$ such that $\theta_j^* = \mathbb{1}_S(j)$.
- Draw samples $x \in \mathbb{R}^p$, *i.i.d* from $\mathbb{P}_X = 0.5\mathbb{P}_1 + 0.5\mathbb{P}_0$ where $\mathbb{P}_1 := \mathcal{N}(\mu_1, \Sigma_\rho)$, $\mathbb{P}_0 := \mathcal{N}(\mu_2, \Sigma_\rho)$. More concretely, firstly draw $u \sim \text{Ber}(0.5)$. If $u = 1$, draw x from \mathbb{P}_1 and draw x from \mathbb{P}_0 otherwise.

² Mean vectors $\mu_1, \mu_2 \in \mathbb{R}^p$ are chosen so that they are s -sparse, i.e. $\text{supp}(\mu_i) =$

²available at <http://www.ms.k.u-tokyo.ac.jp/software.html>

S , $E[\|\mu_1 - \mu_2\|_2^2] = d^2$ and variance of μ_i does not depend on d . Specifically, we sample μ_1, μ_2 such that for $j \in S$, we let $\mu_{1j} \sim \mathcal{N}(\sqrt{(2d^2 - 1)/8s}, 1/\sqrt{8s})$, $\mu_{2j} = -\mu_{1j}$, and for $j \notin S$, $\mu_{ij} = 0$ for $i \in (1, 2)$.

– A covariance matrix $\Sigma_\rho \in \mathbb{R}^{p \times p}$ is taken to be $\Sigma_{\rho,ij} = K_\rho \rho^{|i-j|}$ where K_ρ is chosen so that $\mathbb{1}_S^T \Sigma_\rho \mathbb{1}_S = s$. This scaling of Σ_ρ is made to ensure that the signal strength $\text{Var}(x^T \theta^*) = \mathbb{1}_S^T \Sigma_\rho \mathbb{1}_S$ stays the same across ρ .

- Draw responses $y \in \{0, 1\}$. If scheme = logistic, we draw y such that $y \sim \text{Ber}(\mathbb{P}_{\theta^*}(y = 1|x))$ where $\mathbb{P}_{\theta^*}(y = 1|x) = 1/(1 + \exp(-\theta^{*T} x))$. In contrast, if scheme = mis-specified, we let $y = 1$ if x was drawn from \mathbb{P}_1 , and zero otherwise; i.e. $y = \mathbb{1}\{u = 1\}$.

To compare performances both in low and high dimensional setting, we consider ($p = 10, s = 5$) and ($p = 5000, s = 5$). We set the sample size $n_\ell = n_u = 500$ in both cases. Auto-correlation level ρ takes values in $(0, 0.2, 0.4, 0.6, 0.8)$. In the high dimensional setting, we excluded algorithm (v), since (v) requires a grid search over two dimensions, which makes the computational cost prohibitive. For algorithms (i)-(iv), tuning parameters λ are chosen based on the 10-fold cross validation.

4.3 Classification comparison

We use two criteria, mis-classification rate and F_1 score, to evaluate performances. F_1 is the harmonic mean of the precision and recall, which is calculated as $F_1 := 2 \cdot \frac{\text{precision} + \text{recall}}{\text{precision} \cdot \text{recall}}$. The F_1 score ranges from 0 to 1, where 1 corresponds to perfect precision and recall. Experiments are repeated 50 times and the average score and standard errors are reported. The result for the mis-classification rate under correct model specification is displayed in Figure 3.

Not surprisingly the oracle estimator has the best accuracy in all cases. PUlasso and algorithm (vi) performs almost as well as the oracle in the low-dimensional setting and

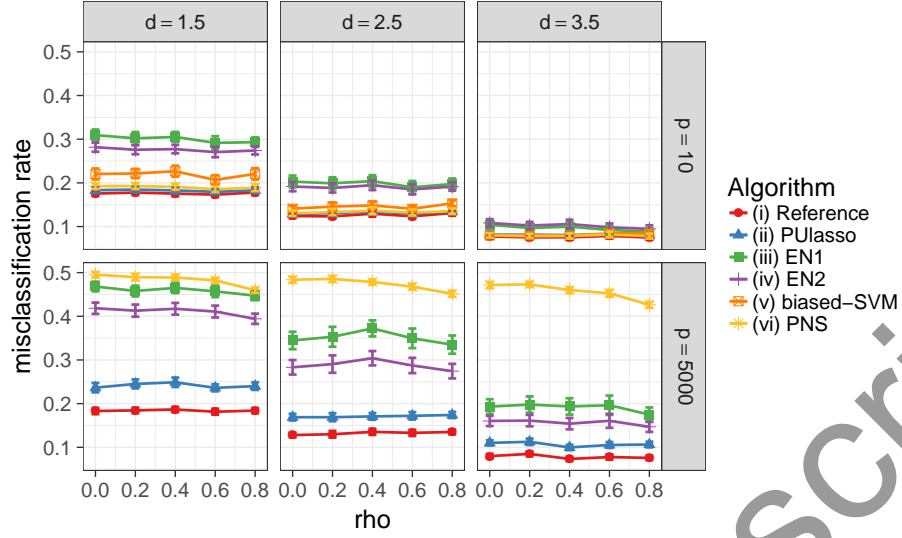


Figure 3: Mis-classification rates of algorithms (i)-(vi) under correct (logistic) model specification. Each error bar represents two standard errors of the mean.

better than remaining methods in most cases. It must be pointed out that both PULasso and algorithm (vi) use additional knowledge π of the true prevalence in the unlabeled samples. PULasso performs best in the high-dimensional setting while the performance of algorithm (vi) becomes significantly worse because estimation errors can be greatly reduced by imposing many 0's on the estimates in PULasso due to the ℓ_1 -penalty (compared to ℓ_2 -penalty in algorithm (vi)). The performance of (iii)-(iv) are greatly improved when positive and negative samples are more separated (large d), because algorithms (iii)-(iv) assume disjoint support between two distributions. The algorithms show similar performance when evaluated with the F_1 score metric and in the mis-specified setting. Due to space constraints, we defer the full set of remaining results in the supplementary material Section S3.

5 Analysis of beta-glucosidase sequence data

Our original motivation for developing the PULasso algorithm was to analyze a large-scale dataset with positive and unlabeled responses developed by the lab of Dr. Philip Romero (Romero et al. (2015)). The prior EM algorithm approach of Ward et al. (2009) did not scale to the size of this dataset. In this section, we discuss the performance of our PULasso algorithm on a dataset involving mutations of a natural beta-glucosidase (BGL) enzyme. To provide context, BGL is a hydrolytic enzyme involved in the deconstruction of biomass into fermentable sugars for biofuel production. Functionality of the BGL enzyme is measured in terms of whether the enzyme deconstructs disaccharides into glucose or not. Dr. Romero used a microfluidic screen to generate a BGL dataset containing millions of sequences (Romero et al. (2015))³.

Main effects and two-way interaction models are fitted using our PULasso algorithm with ℓ_1 and ℓ_1/ℓ_2 penalties (we discuss how the groups are chosen shortly) over a grid of λ values. We test stability of feature selection and classification performance using a modified ROC and AUC approach. Finally a scientific validation is performed based on a follow-up experiment conducted by the Romero lab. The variables selected by PULasso were used to design a new BGL enzyme and the performance is compared to the original BGL enzyme.

5.1 Data description

The dataset consists of $n_\ell = 2647877$ labeled and functional sequences and $n_u = 1567203$ unlabeled sequences where each of the observation $\sigma = (\sigma_1, \dots, \sigma_{500})$ is a sequence of amino acids of length $d = 500$. Each of the position $\sigma_j \in (A, R, \dots, V, *)$ takes one of $M = 21$ discrete values, which correspond to the 20 amino acids in the DNA code and an extra to include the possibility of a gap(*).

³The raw data is available in <https://github.com/RomeroLab/seq-fcn-data.git>

Another important aspect of the millions of sequences generated is that a “base wild-type BGL sequence” was considered and known to be functional ($y = 1$), and the millions of sequences were generated by *mutating* the base sequence. Single mutations (changing one position from the base sequence) and double mutations (changing two positions) from the base sequence were common but higher-order mutations were not prevalent using the deep mutational scanning approach in Romero et al. (2015). Hence the sequences generated were not random samples across the entire enzyme sequence space, but rather very local sequences around the wild-type sequence. Hence the number of possible mutations in each position and consequently the total number of observed sequences is also reduced dramatically. With this dataset, we want to determine which mutations should be applied to the wild-type BGL sequence.

Categorical variables σ are converted into indicator variables: $x = (\mathbb{1}\{\sigma_j = l\})_{j,l}$ where $1 \leq j \leq 500, l \in (A, R, \dots, V, *) \setminus (\sigma_l^{WT})$ for the main-effects model, $x = (\mathbb{1}\{\sigma_j = l\}, \mathbb{1}\{\sigma_j = l, \sigma_k = m\})_{j,k,l,m}$ where $1 \leq j, k \leq 500, j \neq k, l, m \in (A, R, \dots, V, *) \setminus (\sigma_{l \text{ or } m}^{WT})$ for the pair-wise interaction models, where σ_l^{WT} represents the amino acid of the wild-type sequence at the l th position. In other words, each variable corresponds to an indicator of mutation from the base sequence or interaction between mutations. Although there are in principle $p \approx d(M - 1)$ variables for a main-effects model and $p \approx d^2(M - 1)^2$ if we include main-effects and two-way interactions, there are many amino acids that never appear in any position or appear only a small number of times. For features corresponding to the main-effects ($\mathbb{1}\{\sigma_j = l\}$ for some j and l), those sparse features are aggregated *within* each position until the number of mutations of the aggregated column reaches 100 or 1% of the total number of mutations in each position; accordingly, each aggregated column is an indicator of any mutations to those sparse amino acids. For two-way interactions features ($\mathbb{1}\{\sigma_j = l, \sigma_k = m\}$ for some j, k, l , and m), sparse features (≤ 25 out of 4215080 samples) are simply removed from the feature space. Using this basic pre-processing we ob-

tained only 3075 corresponding to single mutations and 930 binary variables corresponding to double mutations. They correspond to 500 unique positions and 820 two-way interactions between positions respectively. As mentioned earlier, we consider both ℓ_1 and group ℓ_1/ℓ_2 penalties. We use the ℓ_1 -penalty for the main-effects model and the ℓ_1/ℓ_2 for the two-way interaction models. For the two-way interaction model each group g_j corresponds to a different position (500 total) and pair of positions (820 total) where mutations occur in the pre-processed design matrix and the group size $|g_j|$ corresponds to the number of different observed mutations in each position or pair of mutations in pair of positions (for this dataset $m = \max_j |g_j| = 8$). Higher-order interactions were not modeled as they did not frequently arise. Hence the main-effects and two-way interaction model we consider have $p = 3076$ ($1 + 3075$) and $p = 4006$ ($1 + 3075 + 930$) and $J = 1320$ ($500 + 820$) groups respectively. In summary, we consider the following two models and corresponding design matrices

$$X_{main} := [\text{Intercept}(1) + \text{main effects}(3075)] \in \{0, 1\}^{4215080 \times 3076}$$

$$X_{int} := [\text{Intercept}(1) + \text{main effects}(3075) + \text{two way interactions}(930)] \in \{0, 1\}^{4215080 \times 4006}$$

and the response vector $z = [1, \dots, 1, 0, \dots, 0]^T \in \{0, 1\}^{4215080}$.

5.2 Classification validation and model stability

Next we validate the classification performance for both the main-effect and two-way interaction models. We fit models using 90% of the randomly selected samples both from the positive and unlabeled set and use Area Under the ROC Curve (AUC) to evaluate the classification performance on the 10% of the hold-out set. Since positive and negative samples are mixed in the unlabeled test dataset this is a non-trivial task with presence-only responses. A naive approach is to treat unlabeled samples as negative and estimate AUC, but if we do so, the AUC is inevitably downward-biased because of the inflated false positive (FP)

rate. We note that a true positive (TP) rate can be estimated in an unbiased manner using positive samples. To adjust such bias, we follow the methodology suggested in Jain et al. (2017) and adjust false positive rate and AUC value using the following equation:

$$FP^{adj} = \frac{FP^{naive} - \pi TP}{1 - \pi}, \quad AUC^{adj} = \frac{AUC^{naive} - \pi/2}{1 - \pi}$$

where π is the prevalence of positive samples.

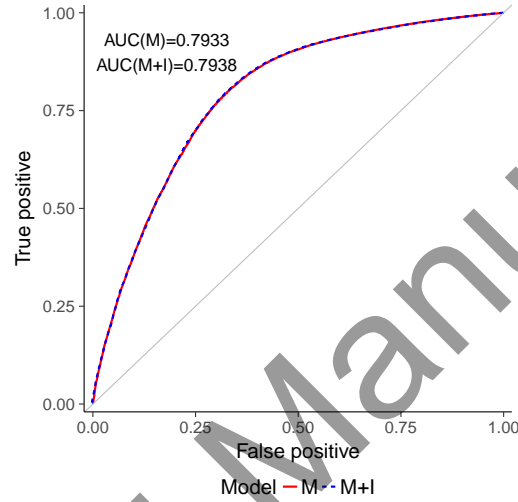


Figure 4: ROC curves of main effects (M) and two-way interaction model (M+I) with λ chosen based on 10-fold cross validation.

As Fig. 4 shows, we have a significant improvement in AUC over random assignment ($AUC=0.5$) in both the main effect ($AUC=0.7933$) and two-way interaction ($AUC=0.7938$) models. The performances of the two models in terms of AUC values are very similar at their best λ values chosen by 10-fold cross validation. This is not very surprising as only a small number of two-way interactions are observed in the experiments.

We also examined the stability of the selected features for both models as the training

data changes. Following the methodology of Kalousis et al. (2007), we measure similarity between two subsets of features s, s' using $S_S(s, s')$ defined as $S_S(s, s') := 1 - \frac{|s| + |s'| - 2|s \cap s'|}{|s| + |s'| - |s \cap s'|}$. S_S takes values in $[0, 1]$, where 0 means that there is no overlap between the two sets, and 1 that the two sets are identical. S_s is computed for each pair of two training folds (i.e. we have $\frac{9-10}{2}$ pairs) using selected features and computed values are finally averaged over all pairs. Feature selection turned out to be very stable across all tuning parameter λ values: on average we had about 95% overlap of selection in main effect model (M) and about 98% overlap in main effect+interaction model (M+I). Stability score is higher in the latter model since we do a feature selection on groups, whose number is much less than individual variables (1320 groups versus 3076 individual variables).

	1st Qu.	Median	Mean	3rd Qu.
M	93.3%	94.9%	94.9%	96.8%
M+I	97.9%	98.8%	98.4%	99.3%

Table 3: Summary of stability scores across all tuning parameter λ values

5.3 Scientific validation: Designed BGL sequence

Finally we provide a scientific validation of the mutations estimated by our PULasso algorithm. In particular, we fit the model with the PULasso algorithm and selected the best $\lambda = 0.0001$ based on the 10-fold cross validation. We use the top 10 mutations based on the largest size of coefficients with positive signs from our PULasso algorithm because we are interested in mutations that enhance the performance of the sequence. Dr. Romero’s lab designed the BGL sequence with the 10 positive mutations from Table 4. This sequence was synthesized, expressed, and assayed for its hydrolytic activity. Hence the designed sequence has 10 mutations compared to the wild-type (base) BGL sequence.

Figure 5 shows firstly that the designed protein sequence folds which in itself is re-

markable given that 10 positions are mutated. Secondly Figure 5 shows that the designed sequence decomposes disaccharides into glucose more quickly than the wild-type sequence. These promising results suggest that our variable selection method is able to identify positions of the wild-type sequences with improved functionality.

Base/Position/Mutated	
T197P	E495G
K300P	A38G
G327A	S486P
A150D	T478S
D164E	D481N

Table 4: Ten positive mutations

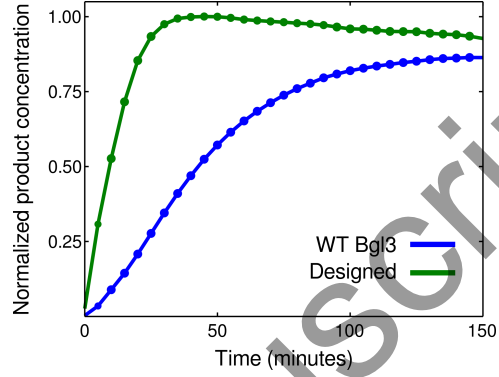


Figure 5: kinetics

10 positive mutations used in the lab(Base state/Position/Mutated state) and kinetics of designed BGL enzyme versus wild-type (WT) BGL sequence. The designed BGL enzyme based on mutations from Table 4 displays faster kinetics than the WT BGL sequence.

6 Conclusion

In this paper we developed the PULasso algorithm for both variable selection and classification for high-dimensional classification with presence-only responses. Theoretically, we showed that our algorithm converges to a stationary point and every stationary point within a local neighborhood of θ^* achieves an optimal mean squared error (up to constant). We also demonstrated that our algorithm performs well on both simulated and real data. In particular, our algorithm produces more accurate results than the existing techniques in simulations and performs well on a real biochemistry application.

References

- M. Blazre, J. M. Loubes, and F. Gamboa. Oracle Inequalities for a Group Lasso Procedure Applied to Generalized Linear Models in High Dimension. *IEEE Transactions on Information Theory*, 60(4):2303–2318, April 2014.
- Patrick Breheny and Jian Huang. Group descent algorithms for nonconvex penalized linear and logistic regression models with grouped predictors. *Statistics and Computing*, 25(2):173–187, 2013.
- Plessis Du Marthinus, Gang Niu, and Masashi Sugiyama. Convex Formulation for Learning from Positive and Unlabeled Data. *Proceedings of The 32nd International Conference on Machine Learning*, pages 1386–1394, 2015.
- Charles Elkan and Keith Noto. Learning Classifiers from Only Positive and Unlabeled Data. In *Proceedings of the 14th ACM SIGKDD International Conference on Knowledge Discovery and Data Mining*, KDD ’08, pages 213–220, New York, NY, USA, 2008. ACM.
- Andreas Elsener and Sara van de Geer. Sharp oracle inequalities for stationary points of nonconvex penalized m-estimators. February 2018.
- Ludwig Fahrmeir and Heinz Kaufmann. Consistency and Asymptotic Normality of the Maximum Likelihood Estimator in Generalized Linear Models. *The Annals of Statistics*, 13(1):342–368, March 1985.
- Douglas M Fowler and Stanley Fields. Deep mutational scanning: a new style of protein science. *Nature Methods*, 11:801–807, 2014.
- Jerome Friedman, Trevor Hastie, Holger Hfling, and Robert Tibshirani. Pathwise coordinate optimization. *The Annals of Applied Statistics*, 1(2):302–332, 2007.

- Jerome Friedman, Trevor Hastie, and Robert Tibshirani. Regularization Paths for Generalized Linear Models via Coordinate Descent. *Journal of Statistical Software*, 33(1), 2010.
- Ryan T Hietpas, Jeffrey D Jensen, and Daniel N A Bolon. Experimental illumination of a fitness landscape. *Proceedings of the National Academy of Sciences of the United States of America*, 108(19):7896–7901, 2011.
- Jian Huang, Patrick Breheny, and Shuangge Ma. A Selective Review of Group Selection in High-Dimensional Models. *Statistical Science*, 27(4):481–499, November 2012.
- Shantanu Jain, Martha White, and Predrag Radivojac. Recovering True Classifier Performance in Positive-Unlabeled Learning. In *Proceedings of the Thirty-First AAAI Conference on Artificial Intelligence, February 4-9, 2017, San Francisco, California, USA.*, pages 2066–2072, 2017.
- Sham Kakade, Ohad Shamir, Karthik Sindharan, and Ambuj Tewari. Learning Exponential Families in High-Dimensions: Strong Convexity and Sparsity. In *Proceedings of the Thirteenth International Conference on Artificial Intelligence and Statistics*, pages 381–388, March 2010.
- Alexandros Kalousis, Julien Prados, and Melanie Hilario. Stability of Feature Selection Algorithms: A Study on High-dimensional Spaces. *Knowl. Inf. Syst.*, 12(1):95–116, May 2007.
- B. Krishnapuram, L. Carin, M. A. T. Figueiredo, and A. J. Hartemink. Sparse multinomial logistic regression: fast algorithms and generalization bounds. *IEEE Transactions on Pattern Analysis and Machine Intelligence*, 27(6):957–968, June 2005.
- Tony Lancaster and Guido Imbens. Case-control studies with contaminated controls. *Journal of Econometrics*, 71(1):145–160, 1996.

- Kenneth Lange, David R. Hunter, and Ilsoon Yang. Optimization Transfer Using Surrogate Objective Functions. *Journal of Computational and Graphical Statistics*, 9(1):1–20, 2000.
- Su-in Lee, Honglak Lee, Pieter Abbeel, and Andrew Y. Ng. Efficient l1 regularized logistic regression. In *In Proceedings of the Twenty-first National Conference on Artificial Intelligence (AAAI-06)*, pages 1–9, 2006.
- Bing Liu, Yang Dai, Xiaoli Li, Wee Sun Lee, and Philip Yu. Building Text Classifiers Using Positive and Unlabeled Examples. *Proceedings of the Third IEEE International Conference on Data Mining (ICDM'03)*, 2003.
- P-L. Loh and M. J. Wainwright. Regularized M-estimators with nonconvexity: Statistical and algorithmic theory for local optima. *Journal of Machine Learning Research*, 1:1–9, 2013.
- P. McCullagh and J. A. Nelder. *Generalized Linear Models*, volume 28. 1989.
- Song Mei, Yu Bai, and Andrea Montanari. The landscape of empirical risk for nonconvex losses. *Ann. Stat.*, 46(6A):2747–2774, December 2018.
- Lukas Meier, Van De S Geer, Peter Buhlmann, Sara Van De Geer, and Peter Bhlmann. The group lasso for logistic regression. *Journal of the Royal Statistical Society, Series B*, 70(1):53–71, 2008.
- S. N. Negahban, R. Pradeep, Bin Yu, and M. J. Wainwright. A Unified Framework for High-Dimensional Analysis of M-Estimators with Decomposable Regularizers. *Statistica Sinica*, 27(4):538–557, 2012.
- J. M. Ortega and W. C. Rheinboldt. *Iterative solution of nonlinear equations in several variables*. Classics in applied mathematics. SIAM, New York, 2000.

- A. T. Puig, A. Wiesel, G. Fleury, and A. O. Hero. Multidimensional Shrinkage-Thresholding Operator and Group LASSO Penalties. *IEEE Signal Processing Letters*, 18(6):363–366, June 2011.
- G. Raskutti, M. J. Wainwright, and B. Yu. Restricted eigenvalue conditions for correlated Gaussian designs. *Journal of Machine Learning Research*, 11:2241–2259, 2010.
- Garvesh Raskutti, Martin J. Wainwright, and Bin Yu. Minimax Rates of Estimation for High-Dimensional Linear Regression Over ℓ_q -Balls. *IEEE Transactions on Information Theory*, 57(10):6976–6994, October 2011.
- Philip A Romero, Tuan M Tran, and Adam R Abate. Dissecting enzyme function with microfluidic-based deep mutational scanning. *Proceedings of the National Academy of Sciences of the United States of America*, 112(23):7159–7164, 2015.
- Noah Simon and Robert Tibshirani. Standardization and the Group Lasso Penalty. *Statistica Sinica*, 22(3):1–21, 2012.
- Robert Tibshirani, Jacob Bien, Jerome Friedman, Trevor Hastie, Noah Simon, Jonathan Taylor, and Ryan J. Tibshirani. Strong rules for discarding predictors in lasso-type problems. *Journal of the Royal Statistical Society. Series B: Statistical Methodology*, 74(2):245–266, 2012.
- Sara A. van de Geer. High-dimensional generalized linear models and the lasso. *The Annals of Statistics*, 36(2):614–645, April 2008.
- Gill Ward, Trevor Hastie, Simon Barry, Jane Elith, and John R. Leathwick. Presence-only data and the em algorithm. *Biometrics*, 65(2):554–563, 2009.
- Tong Tong Wu and Kenneth Lange. Coordinate descent algorithms for lasso penalized regression. *The Annals of Applied Statistics*, 2(1):224–244, 2008.

Ming Yuan and Yi Lin. Model selection and estimation in regression with grouped variables.
J. R. Statist. Soc. B, 68(1):49–67, 2006.

Accepted Manuscript